Supplement of Atmos. Chem. Phys., 20, 5071–5092, 2020
https://doi.org/10.5194/acp-20-5071-2020-supplement

Atmospheric Chemistry and Physics
Open Access

Supplement of

High-resolution vertical distribution and sources of HONO and NO_2 in the nocturnal boundary layer in urban Beijing, China

Fanhao Meng et al.

Correspondence to: Min Qin (mqin@aiofm.ac.cn)

Table S1. The date, time and meteorological conditions for each vertical profile measurements in this study.

Date	Weather condition	Height (m)	Starting time Ascent	Ending time, Ascent	Starting time, Descent	Ending time, Descent
7/12/2016	Haze (E1)	240	22:42:00	23:07:00	23:25:09	23:49:39
9/12/2016	Clean (C2)	240	17:13:12	17:38:14	17:47:35	18:12:06
9/12/2016	Clean (C2)	240	22:42:04	23:06:59	23:15:48	23:40:13
10/12/2016	Clean (C2)	240	17:15:09	17:40:05	17:49:24	18:13:51
10/12/2016	Clean (C2)	240	22:36:29	23:01:21	23:01:21	23:25:43
11/12/2016	Haze (E3)	240	18:16:21	18:41:14	18:50:17	19:14:41
11/12/2016	Haze (E3)	240	22:35:29	23:00:19	23:04:19	23:28:54
12/12/2016	Haze (E3)	240	00:00:39	00:25:54	00:45:05	01:09:34

Table S2. Comparison of emission ratios ($HONO/NO_x$) in various studies.

Studied object	$HONO/NO_x$ (%)	Description	Reference
Caldecott Tunnel (United States)	0.24–0.38	Traffic fleet composition: more than 99% gasoline-fueled and less than 0.2% heavy-duty vehicles	Kirchstetter et al. (1996)
Kiesbergtunnel (Germany)	0.8 ± 0.1	Traffic fleet composition: ~75% gasoline-fueled car and 6% heavy-duty trucks	Kurtenbach et al. (2001)
MAN truck	0.53 ± 0.08	Diesel engine; tested under the speeds of 0-40 km h^{-1} over a distance of 3500 m	
VW-Golf gasoline car	0.65 ± 0.24	Equipped with three-way-catalyst; tested under the speeds of 0-40 km h^{-1} over a distance of 3500 m	
VW-Golf diesel car	0.66 ± 0.20	Equipped with oxidation catalyst; tested under the speeds of 0-40 km h^{-1} over a distance of 3500 m	
Xinken (China)	1.0	Estimation of direct emission of HONO from the fresh emission (NO> 20 ppb); the minimum HONO/NOx was treated as emission factor	Su et al. (2008)
Back Garden (China)	1.8	Estimation of direct emission of HONO from the fresh emission (NO> 20 ppb); the minimum HONO/NOx was treated as emission factor	Li et al. (2012)
Highway junction in Houston (United States)	1.70 ± 0.09	Daily traffic volume was 400,000 vehicles; 5-10% among them were heavy-duty diesel vehicles	Rappengluck et al. (2013)
Beijing tunnel	2.1		Yang et al. (2014)
Tung Chung (Hong Kong)	0.5–1.6	Estimation of direct emission of HONO from 21 fresh plumes (NO/NO_x> 0.8). Measurement site was very close to the TC Expressway (80 m). Traffic fleet composition: 33% of diesel and 67% gasoline vehicles	Xu et al. (2015)
Shing Mun Tunnel (China)	1.26 ± 0.34	Traffic fleet composition: 47% gasoline vehicles, 38% diesel vehicles and 15% Liquefied Petroleum Gas (LPG) vehicles	Liang et al. (2017)
Beijing (China)	1.3	Estimation of direct emission of HONO from the fresh emission (NO> 20 ppb); the minimum HONO/NOx was treated as emission factor. Measurement site is about 480 m away from the Fourth Ring Road	Zhang et al. (2018)
Ji'nan (China)	0.19–0.87	Estimation of direct emission of HONO from 12 fresh plumes (NO/NO_x >0.7). Measurement site close to several main traffic roads	Li et al. (2018)
Suburb of Nanjing (China)	0.26–1.91	Estimation of direct HONO from 55 fresh plumes (NO/NO_x>0.85). The air masses at measurement site are influenced by both industries and vehicles.	Liu et al. (2019)
Beijing (China)	0.78–1.73	Estimation of direct emission of HONO from 11 fresh plumes; only sharp peaks and the elevations of HONO and NOx over background levels were estimated. Measurement site is surrounded by several traffic roads	This work

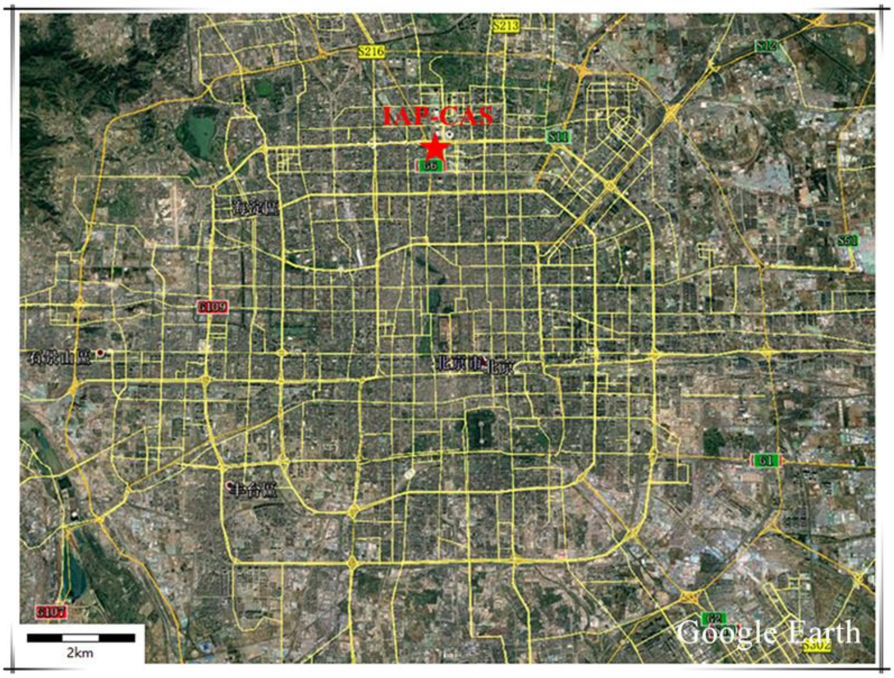

Figure S1. Map of the measurement site (Tower Branch of the Institute of Atmospheric Physics (IAP), Chinese Academy of Sciences (CAS)) shows the location of the Beijing 325- m meteorological tower (BMT). The map is adapted from © Google Earth 2019.

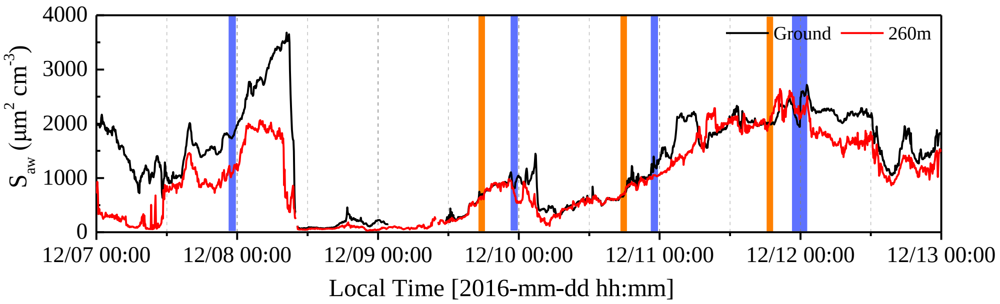

Figure S2. Time series of RH corrected aerosol surface density (S_{aw}) at ground level and at 260 m at IAP-Tower Division in Beijing from December 7th to 12th of 2016. The shaded regions represent the vertical measurements.

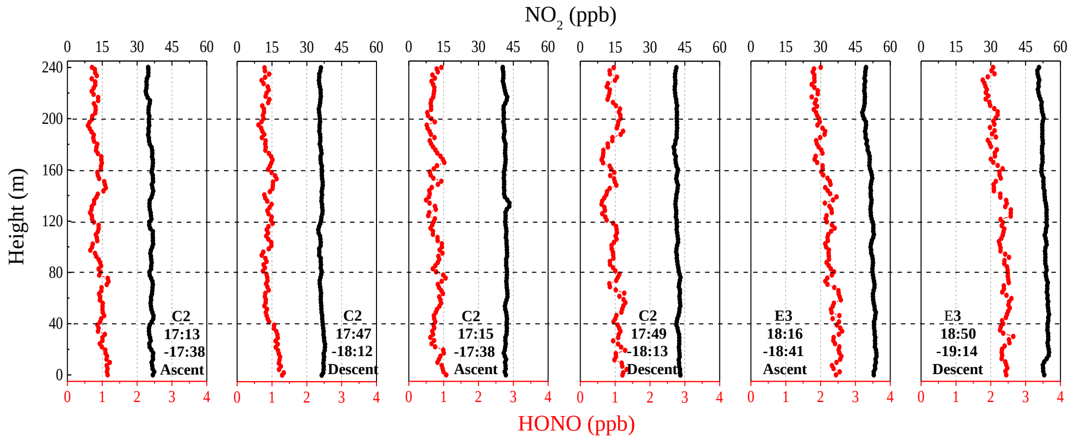

Figure S3. Vertical profiles of HONO (red solid line) and NO_2 (black solid line) after sunset during the clean episode (C2) and the haze episode (E3). Each vertical measurement includes an ascent process and a descent process. The time on each plot corresponds to the measurement time for each vertical profile.

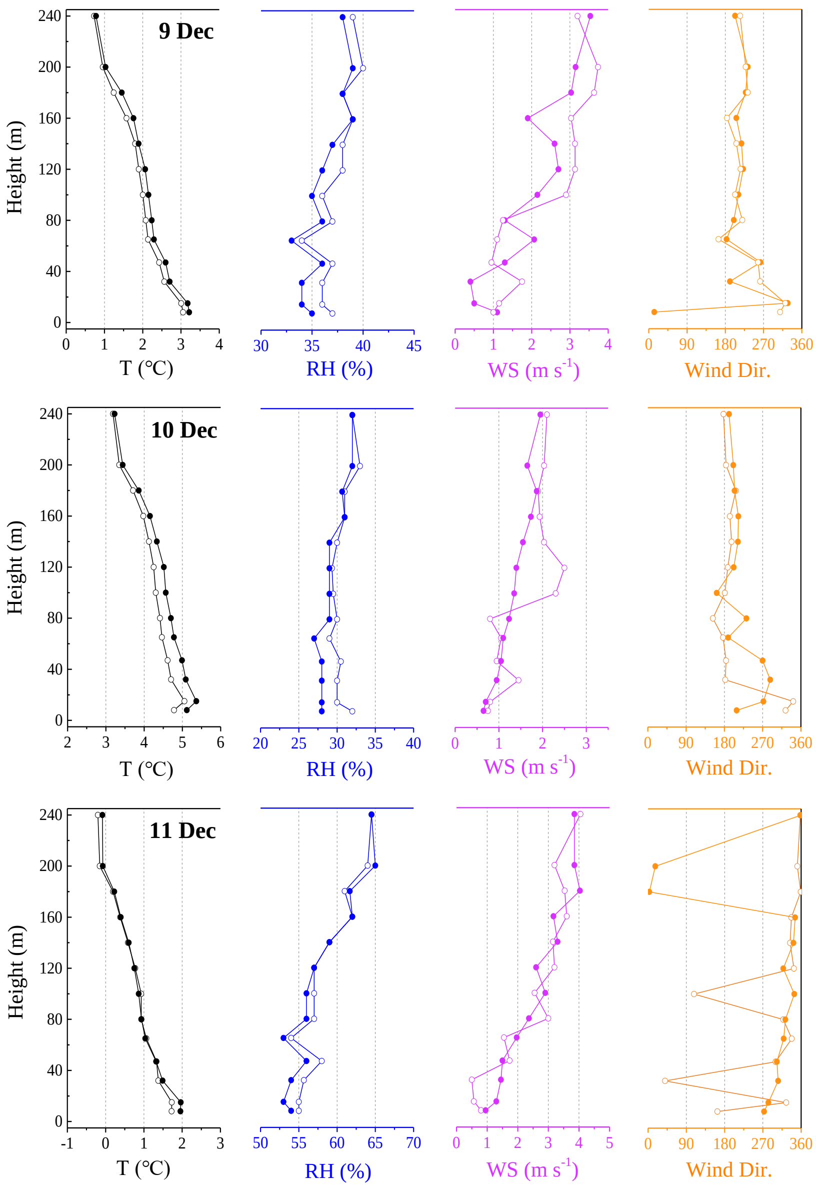

Figure S4. Vertical profiles of temperature (T), relative humidity (RH), wind speed (WS), and wind direction (WD) after sunset on December 9th, 10th, and 11th. The solid circle represents ascent profiles while others are descent profiles.

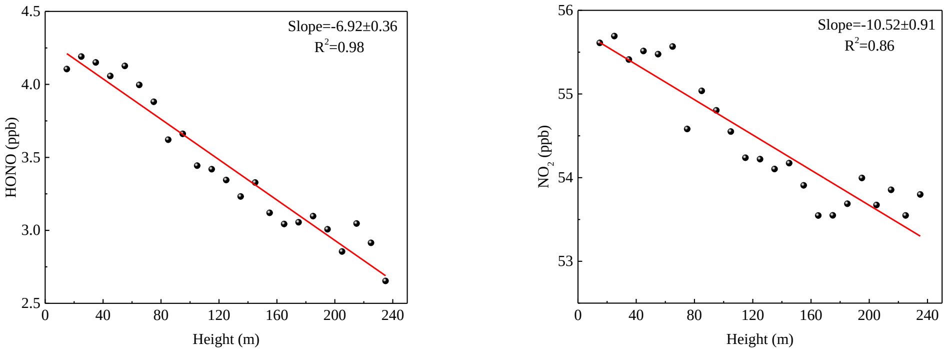

Figure S5. The linear least squares regression of HONO and NO_2 to altitude on December 11th as an example of evaluation of the vertical gradient of HONO and NO_2 at night.

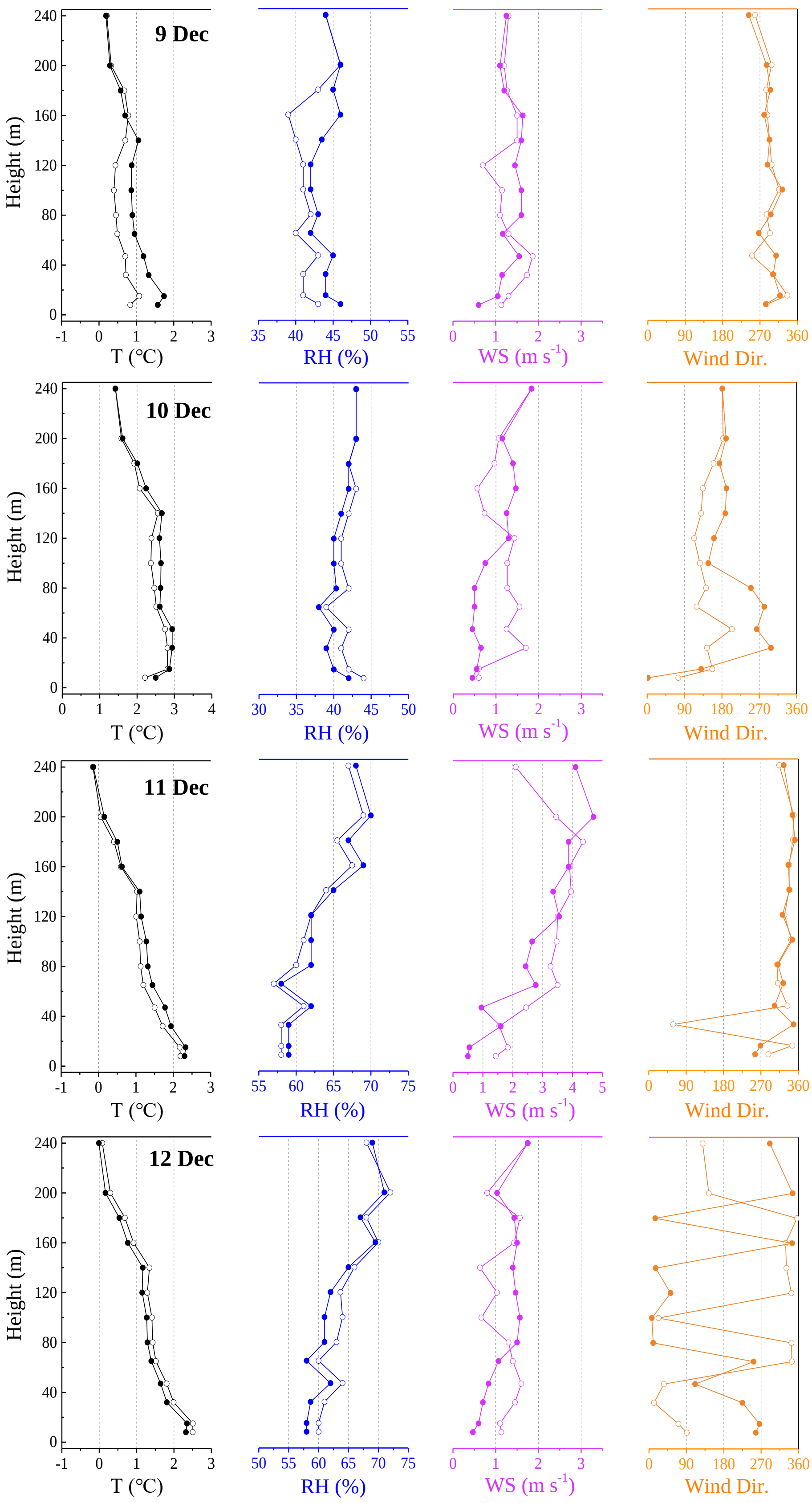

Figure S6. Vertical profiles of temperature (T), relative humidity (RH), wind speed (WS), and wind direction (WD) on the nighttime of December 9th, 10th, and 11th and midnight of December 12th. The solid circle represents ascent profiles while others are descent profiles.

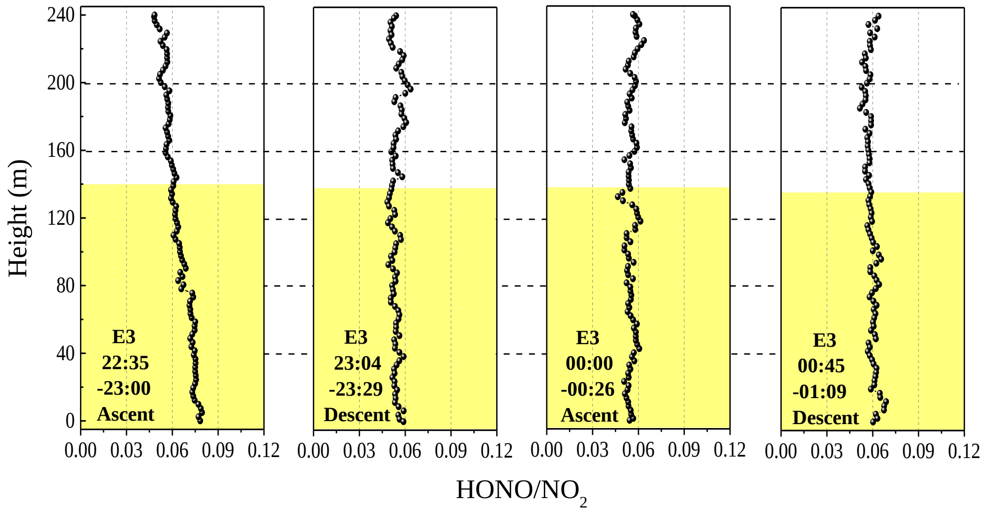

Figure S7. Evolution of the $HONO/NO_2$ vertical profiles from 22:35 to 01:09 LT on December 11th to 12th. The time on each plot corresponds to the measurement time for each vertical profile. The height of the nocturnal boundary layer (NBL) is denoted by the shaded yellow region.

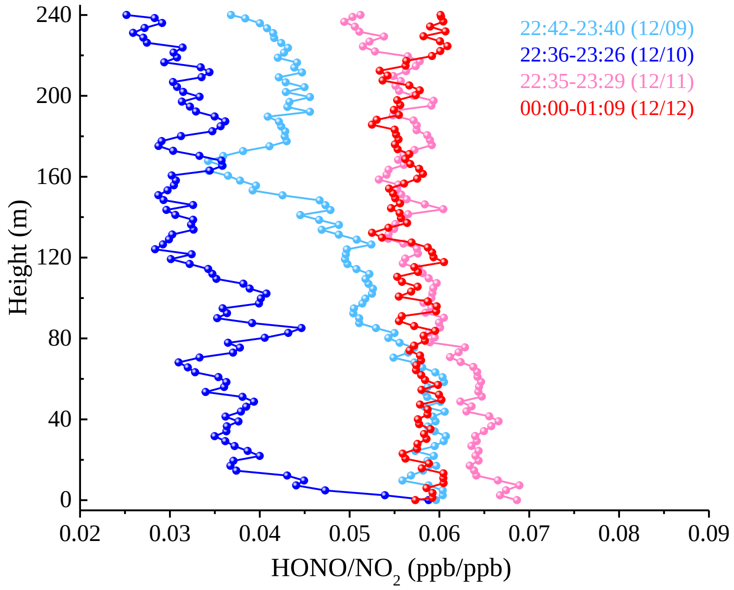

Figure S8. The average vertical profiles of nighttime $HONO/NO_2$ ratio from C2 (12/09 and 12/10) to E3 (12/11 and 12/12). Each trace represents the average $HONO/NO_2$ ratio of an ascent and a descent profile.

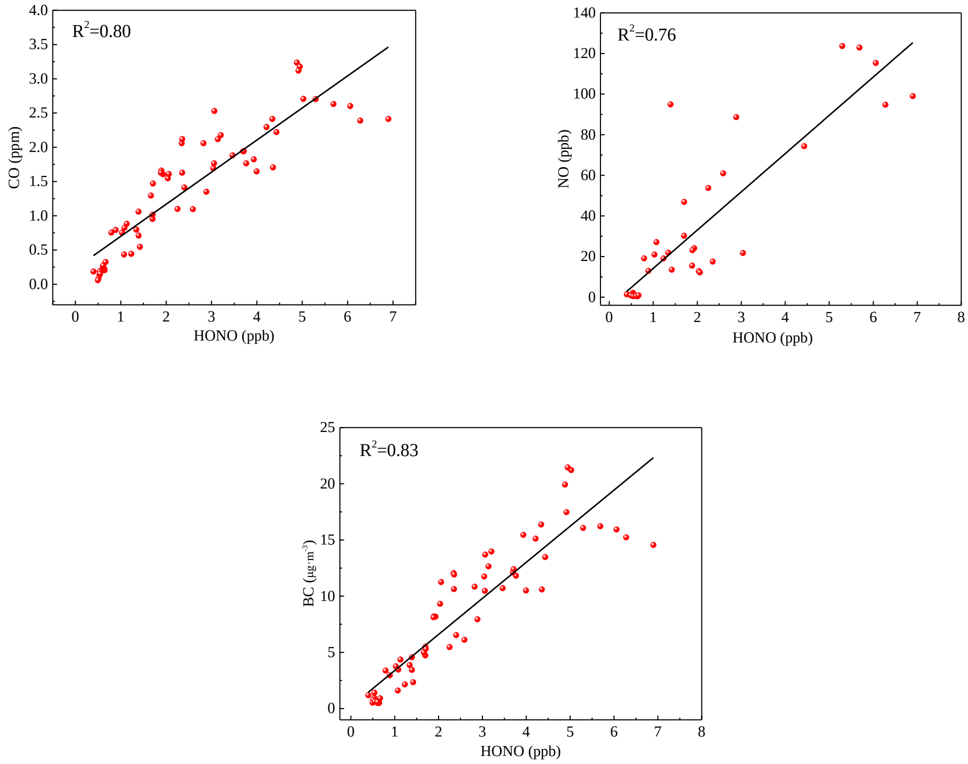

Figure S9. Correlations of HONO with CO, NO, and BC at ground level at night from December 7th to 12th of 2016. The NO data are available before 14:00 on December 10th, 2016.

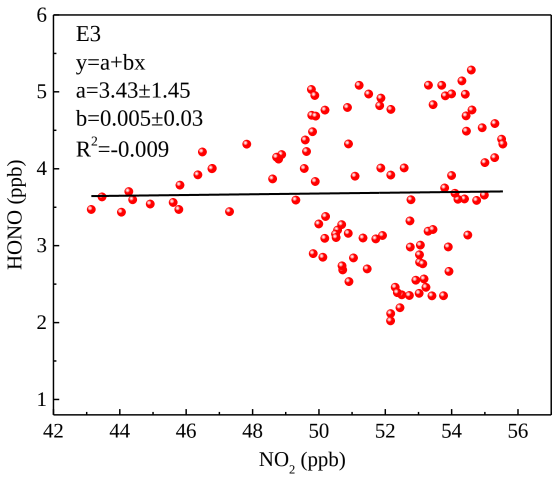

Figure S10. Correlation between HONO and NO_2 at ground level during the haze episode (E3). Only the nocturnal data were used to avoid the influence of photolysis of HONO and NO_2 in the daytime.

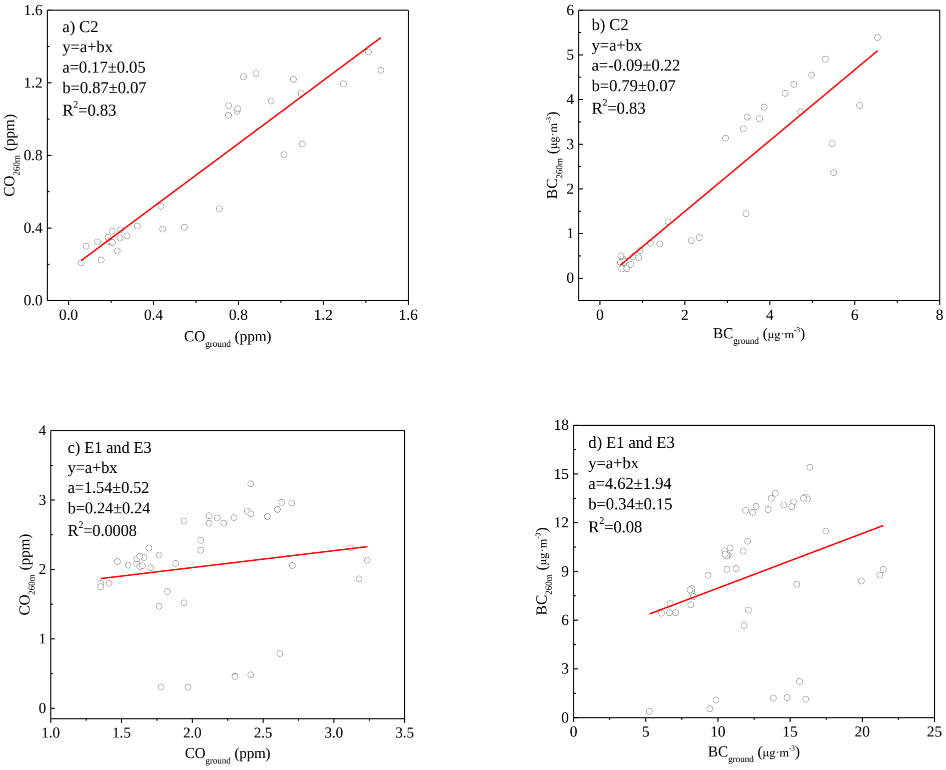

Figure S11. The linear least squares correlation between the observed CO and BC at ground level and the CO and BC measured at 260m at night during (a and b) the clean episode and (c and d) the haze episode.

References supplement:

Kirchstetter, T. W., Harley, R. A., and Littlejohn D.: Measurement of nitrous acid in motor vehicle exhaust, Environ. Sci. Technol., 30, 2843-2849, https://doi.org/10.1021/es960135y, 1996.

Kurtenbach, R., Becker, K. H., Gomes, J. A. G., Kleffmann, J., Lörzer, J., Spittler, M., Wiesen, P., Ackermann, R., Geyer, A., and Platt, U.: Investigations of emission and heterogeneous formation of HONO in a road traffic tunnel, Atmos. Environ., 35, 3385–3394, https://doi.org/10.1016/S1352-2310(01)00138-8, 2001.

Li, D. D., Xue, L. K., Wen, L., Wang, X. F., Chen, T. S., Mellouki, A., Chen, J. M., and Wang, W. X.: Characteristics and sources of nitrous acid in an urban atmosphere of northern China: Results from 1-yr continuous observations, Atmos. Environ., 182, 296-306, https://doi.org/10.1016/j.atmosenv.2018.03.033, 2018.

Liang, Y. T., Zha, Q. Z., Wang, W. H., Cui, L., Lui, K. H., Ho, K. F., Wang, Z., Lee, S. C., and Wang, T.: Revisiting nitrous acid (HONO) emission from on-road vehicles: A tunnel study with a mixed fleet, J. Air Waste Manag., 67, 797-805, https://doi.org/10.1080/10962247.2017.1293573, 2017.

Liu, Y. L., Nie, W., Xu, Z., Wang, T. Y., Wang, R. X., Li, Y. Y., Wang, L., Chi, X. G., and Ding, A. J.: Semi-quantitative understanding of source contribution to nitrous acid (HONO) based on 1 year of continuous observation at the SORPES station in eastern China, Atmos. Chem. Phys., 19, 13289-13308, https://doi.org/10.5194/acp-19-13289-2019, 2019.

Rappenglück, B., Lubertino, G., Alvarez, S., Golovko, J., Czader, B., and Ackermann, L.: Radical precursors and related species from traffic as observed and modeled at an urban highway junction, J. Air Waste Manag. Assoc., 63, 1270-1286, https://doi.org/10.1080/10962247.2013.822438, 2013.

Su, H., Cheng, Y. F., Cheng, P., Zhang, Y. H., Dong, S. F., Zeng, L. M., Wang, X. S., Slanina, J., Shao, M., and Wiedensohler, A.: Observation of nighttime nitrous acid (HONO) formation at a non-urban site during PRIDE-PRD2004 in China, Atmos. Environ., 42, 6219-6232, https://doi.org/10.1016/j.atmosenv.2008.04.006, 2008.

Xu, Z., Wang, T., Wu, J. Q., Xue, L. K., Chan, J., Zha, Q., Z., Zhou, S. Z., Louie, P. K. K., and Luk, C. W. Y.: Nitrous acid (HONO) in a polluted subtropical atmosphere: Seasonal variability, direct vehicle emissions and heterogeneous production at ground surface, Atmos. Environ., 106, 100-109, https://doi.org/10.1016/j.atmosenv.2015.01.061, 2015.

Yang, Q., Su, H., Li, X., Cheng, Y. F., Lu, K. D., Cheng, P., Gu, J. W., Guo, S., Hu, M., Zeng, L. M., Zhu, T., and Zhang, Y. H.: Daytime HONO formation in the suburban area of the megacity Beijing, China, Sci. China Chem., 57, 1032-1042, https://doi.org/10.1007/s11426-013-5044-0, 2014.

Zhang, W. Q., Tong, S. R., Ge, M. F., An, J. L., Shi, Z. B., Hou, S. Q., Xia, K. H., Qu, Y., Zhang, H. X., Chu, B. W., Sun, Y. L., and He, H.: Variations and sources of nitrous acid (HONO) during a severe pollution episode in Beijing in winter 2016, Sci. Total Environ., 648, 253-262, https://doi.org/10.1016/j.scitotenv.2018.08.133, 2018.